Syntheses and Structure of Heterometallic Complexes Containing Tripodal Group 13 Ligands $[RE(2\text{-py})_3]^-$ (E = Al, In)†

Felipe García, Alexander D. Hopkins,* Richard A. Kowenicki, Mary McPartlin, Michael C. Rogers, Jared S. Silvia, and Dominic S. Wright*

Chemistry Department, University of Cambridge, Lensfield Road, Cambridge CB2 1EW, U.K.

Received January 23, 2006

Reactions of the Al(III) complex [{MeAl(2-py)$_3$}Li·THF] (**1**), containing the tripodal [MeAl(2-py)$_3$]$^-$ ligand, with [(C$_7$H$_8$)Mo(CO)$_3$], CaI$_2$, and ZnCl$_2$ give the trimetallic and bimetallic complexes [{MeAl(2-py)$_3$}Mo(CO)$_3$Li(THF)$_3$] (**2**), [{MeAl(2-py)$_3$}$_2$Ca] (**3**), and [{MeAl(2-py)$_3$}ZnCl] (**4**), respectively. [{^{n}BuIn(2-py)$_3$}Li·THF] (**5**), an In^{III} analogue of **1** containing the [^{n}BuIn(2-py)$_3$]$^-$ anion, is obtained by the one-pot reaction of ^{n}BuLi with InCl$_3$ followed by reaction with 2-Li-py. Complex **5** reacts with [(C$_7$H$_8$)Mo(CO)$_3$] to give [{^{n}BuIn(2-py)$_3$}Mo(CO)$_3$Li(THF)$_2$]$_\infty$ (**6**) (analogous to the Al^{III} complex **2**). The X-ray structures of the new complexes **2**, **3**, **4**, **5**, and **6** are reported.

Introduction

Major interest in tris-pyrazolyl-borate and -methane ligands[1] and related tris-pyridyl ligands[2] (Figure 1) has focused on their broad applications in coordination, bioinorganic, and organometallic chemistry as well as in heterogeneous catalysis. Modification of the bridgeheads in these systems provides an obvious way by which the coordination characteristics can be changed, in terms of both their ligand bites and potentially their electronic character as ligands. However, the vast majority of studies of tris-pyridyl ligands reported to date contain nonmetallic main group element bridgeheads, commonly with Y = CX (X = H, OH, OR, NH$_2$), N, P, and P=O.[3−6]

Our interests in this area have involved the development of synthetic routes to tris-pyridyl ligands containing main group *metal* bridgeheads.[7,8] These species usually have greater ligand bites than their nonmetallic counterparts, as a result of the greater

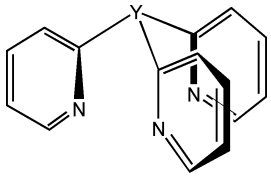

Figure 1. Structure of tris-pyridyl ligands.

Y−C bond lengths. In addition, replacment of nonmetallic bridgehead groups by metallic ones introduces the potential for variable oxidation states at the bridgehead atoms as well as electrochemical activity. The ability for the metal bridgehead to possess various oxidation states was illustrated by the syntheses of the anionic group 14 ligands [^{n}BuSn(2-py)$_3$][7a] and [Pb(2-py)$_3$],[7b] containing metallic bridgehead atoms in the IV and II oxidation states, respectively. An indication of the electrochemical activity of metallic bridgeheads was provided by the reaction of [{^{n}BuSn(2-py)$_3$}LiBr] with Cu^{II}Cl$_2$,[7b] the product being the Cu^I complex [{^{n}BuSn(2-py)$_3$}CuBr], presumably formed by the coupling of 2-py groups into 2,2′-bipyridine.

In more recent studies we have shown that the Al^{III} complex [{MeAl(2-py)$_3$}Li·THF] (**1**) is readily prepared in good yield via the reaction of 2-Li-py with MeAlCl$_2$.[8a] Complex **1** provides a good source of the tripodal [MeAl(2-py)$_3$]$^-$ ligand. We showed, for example, that the reactions of **1** with FeBr$_2$ or Cp$_2$Mn give the bis-coordinate complexes [{MeAl(2-py)}$_2$M] (M

† Dedicated to Prof. Victor Riera (Oviedo University, Spain) on the occasion of his 70th birthday.

* To whom correspondence should be addressed. E-mail: dsw1000@cus.cam.ac.uk. Tel: 0044 1223 763122.

(1) Reger, D. L. *Comments Inorg. Chem.* **1999**, *21*, 1. Trofimenko, S. *Chem. Rev.* **1993**, *93*, 943. Trofimenko, S. *Scorpionates: The Coordination Chemistry of Polypyrazolylborate Ligands*; Imperial College Press: London, 1999.

(2) Szezepura, L. F.; Witham, L. M.; Takeuchi, K. J. *Coord. Chem. Rev.* **1998**, *174*, 5.

(3) For examples involving CH bridgeheads, see: Keene, F. R.; Snow, M. R.; Stephenson, P. J.; Tiekink, E. R. T. *Inorg. Chem.* **1988**, *27*, 2040. Canty, A. J.; Minchin, N. J.; Skelton, B. W.; White, A. H. *Aust. J. Chem. Soc.* **1992**, *45*, 423. Lee, F. W.; Chan, M. C.-W.; Cheung, K.-K.; Che, C.-M. *J. Organomet. Chem.* **1998**, *563*, 191. Kodera, M.; Katayama, K.; Tachi, Y.; Kano, K.; Hirota, S.; Fujinami, S.; Suzuki, M. *J. Am. Chem. Soc.* **1999**, *121*, 11006. Anderson, R. A.; Astley, T.; Hitchman, M. A.; Keene, F. R.; Monbarak, B.; Murray, K. S.; Skelton, B. N.; Tiekink, E. R. T.; Toftland, H.; White, A. H. *J. Chem. Soc., Dalton, Trans.* **2000**, 3505.

(4) For examples involving C(OR), C(NH$_2$) bridgeheads, see: Kanty, A. J.; Chaichit, N.; Gatehouse, B. M.; Goerge, E. E. *Inorg. Chem.* **1981**, *20*, 4293. Keene, F. R.; Szalda, D. J.; Wilson, T. A. *Inorg. Chem.* **1987**, *26*, 2211. Jonas, R. T.; Stack, T. D. P. *Inorg. Chem.* **1998**, *37*, 6615. Brunner, H.; Maier, R. J.; Zabel, M. *Synthesis* **2001**, 2484. Arnold, P. J.; Davies, S. C.; Dilworth, J. R.; Durrant, M. C.; Griffiths, D. V.; Hughs, D. L.; Richards, R. L.; Sharpe, P. C. *J. Chem. Soc., Dalton Trans.* **2001**, 736.

(5) For examples involving N bridgeheads, see: Kucharski, E. S.; McWhinnie, A. H.; White, W. R. *Aust. J. Chem. Soc.* **1978**, *31*, 2647. Anderson, P. A.; Keene, F. R.; Gulbis, J. M.; Tiekink, E. R. T. *Z. Kristallogr.* **1993**, *206*, 275. Mosney, K. K.; de Gala, S. R.; Crabtree, R. H. *Transition Met. Chem.* **1995**, *29*, 595. Wang, W.; Schmider, H.; Wu, Q.; Zhang, Y.-S.; Wang, S. *Inorg. Chem.* **2000**, *39*, 2397.

(6) For examples involving P and P=O bridgeheads, see: Schutte, P. R.; Rettig, S. J.; Joshi, A.; Janes, B. R. *Inorg. Chem.* **1997**, *36*, 5809. Gregorzik, R.; Wirbser, J.; Vahrenkamp, H. *Chem. Ber.* **1992**, *125*, 1575. Espinet, P.; Hernando, R.; Iturbe, G.; Villafane, F.; Orpen, A. G.; Pascual, I. *Eur. J. Inorg. Chem.* **2000**, 1031. Casares, J. A.; Espinet, P.; Martin-Alvarez, J. M.; Espino, G.; Perez-Maurique, M.; Vattier, F. *Eur. J. Inorg. Chem.* **2001**, 289.

(7) (a) Beswick, M. A.; Davies, M. K.; Raithby, P. R.; Steiner, A.; Wright, D. S. *Organometallics* **1997**, *16*, 1109. (b) Beswick, M. A.; Belle, C. J.; Davies, M. K.; Halcrow, M. A.; Raithby, P. R.; Steiner, A.; Wright, D. S. *J. Chem. Soc., Chem. Commun.* **1996**, 2619. (c) Morales, D.; Pérez, J.; Riera, L.; Riera, V.; Miguel, D. *Organometallics* **2001**, *20*, 4517. (d) García, F.; Hopkins, A. D.; Humphrey, S. M.; McPartlin, M.; Rogers, M. C.; Wright, D. S. *Dalton Trans.* **2004**, 361.

(8) (a) García, F.; Hopkins, A. D.; Kowenicki, R. A.; McPartlin, M.; Rogers, M. C.; Wright, D. S. *Organometallics* **2004**, *23*, 3884. (b) Alvarez, C. S.; García, F.; Humphrey, S. M.; Hopkins, A. D.; Kowenicki, R. A.; McPartlin, M.; Layfield, R. A.; Raja, R.; Rogers, M. C.; Woods, A. D.; Wright, D. S. *J. Chem. Soc., Chem. Commun.* **2005**, 198.

10.1021/om0600691 CCC: $33.50
Publication on Web 04/08/2006

Scheme 1

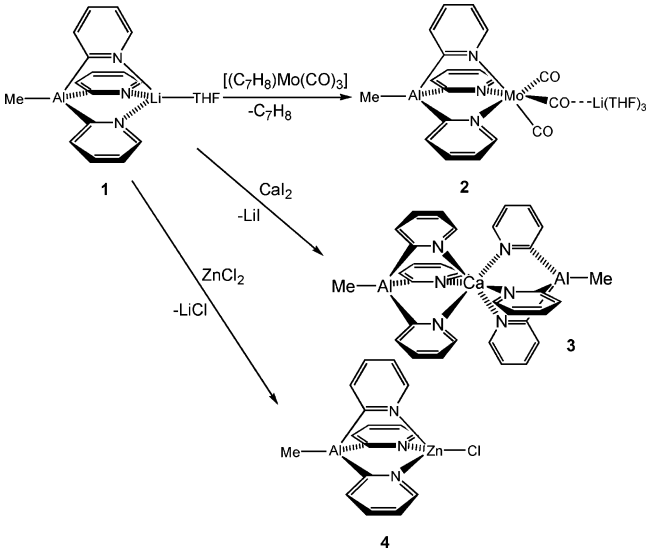

Scheme 2

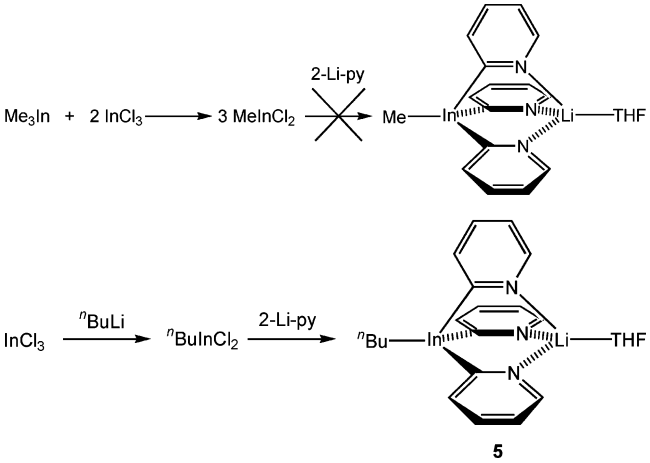

= Fe, Mn).[8b] Such ligand transfer reactions provide a simple approach to well-defined heterometallic group 13 complexes, which have potential applications in catalysis in a number of important areas. For example, it was shown that the Fe^{II} complex [{MeAl(2-py)}$_2$Fe] is the most selective catalyst for the industrially important oxidation of styrene into styrene oxide in air.[8b]

In view of the potentially broad applications of **1** and related group 13 anionic ligands in a range of catalytic systems, it was decided to investigate the coordination chemistry of the [MeAl(2-py)$_3$]$^-$ ligand with a broader range of metals. We present here the syntheses and structures of the new complexes [{MeAl(2-py)$_3$}Mo(CO)$_3$Li(THF)$_3$] (**2**), [{MeAl(2-py)$_3$}$_2$Ca] (**3**), and [{MeAl(2-py)$_3$}ZnCl] (**4**), prepared from metal-exchange reactions of **1** with the appropriate metal sources. We also report the syntheses and structures of [{^{n}BuIn(2-py)$_3$}Li·THF] (**5**) and [{^{n}BuIn(2-py)$_3$}Mo(CO)$_3$Li(THF)$_2$]$_\infty$ (**6**), containing the first In^{III} tris-pyridyl ligand. These studies, together with those of [{MeAl(2-py)}$_2$M] (M = Fe, Mn) communicated previously,[8b] illustrate the broad applications of group 13 tris-pyridyl ligands of this type across the periodic table.

Results and Discussion

The room-temperature reaction of [(C$_7$H$_8$)Mo(CO)$_3$] with [{MeAl(2-py)$_3$Li·THF] (**1**) in THF under dinitrogen occurs rapidly to give a deep red solution, from which the red, trimetallic complex [{MeAl(2-py)$_3$}Mo(CO)$_3$Li(THF)$_3$] (**2**) is isolated in good yield (66%) (Scheme 1). The 1:2 reaction of CaI$_2$ with **1** under nitrogen gives [{MeAl(2-py)$_3$}$_2$Ca] (**3**) (Scheme 1). The disubstitution of the metal center observed here is similar to that observed in the reactions of **1** with FeBr$_2$ and Cp$_2$Mn reported previously.[8b] In contrast, the 1:1 or 1:2 reactions of ZnCl$_2$ with **1** under nitrogen both give the bimetallic Al^{III}/Zn complex [{MeAl(2-py)$_3$}ZnCl] (**4**) after reflux in THF (Scheme 1) (as shown by unit cell analysis of the crystals produced in both reactions). Although the formation of **4** is reproducible, owing to the high solubility of the complex in a range of solvents, only a few crystals of the complex could be isolated. Presumably the smaller size of the Zn^{2+} ion makes coordination by two [MeAl(2-py)$_3$]$^-$ ligands unfavorable both on steric grounds and for reasons of strain within the ligand framework itself [Zn^{2+} 0.88 Å; cf. the ionic radii for bis-coordinated complexes, Ca^{2+} 1.14, Mn^{2+} 0.97, Fe^{2+} 0.92 Å].[9]

Several attempts were made to prepare In^{III} analogues of **1** of the type [RIn(2-py)$_3$Li·THF] via various routes. In particular, the in situ preparation of MeInCl$_2$ from Me$_3$In and InCl$_3$, followed by reaction with 2-Li-py in THF (Scheme 2a), proved to be problematic owing to the apparent instability of the product(s) and the resulting formation of In metal. However, the sequential reaction of InCl$_3$ with ^{n}BuLi followed by reaction with 2-Li-py (Scheme 2b) under nitrogen was successful, giving [{^{n}BuIn(2-py)$_3$}Li·THF] (**5**) as the only isolatable product. The low yield of **5** (only 13%) appears to be mainly the result of decomposition into In metal during its formation. Nonetheless, **5** is stable enough in solution to act as a source of the [^{n}BuIn(2-py)$_3$]$^-$ ligand. Although the reactions of **5** with Cp$_2$Mn or FeBr$_2$ result in extensive decomposition into In metal [cf. the reactions of **1**, which give [{MeAl(2-py)$_3$}$_2$M] (M = Fe, Mn)[8a]], no such decomposition occurs in the reaction of **5** with [(C$_7$H$_8$)Mo(CO)$_3$]. The product [{^{n}BuIn(2-py)$_3$}Mo(CO)$_3$Li(THF)$_2$]$_\infty$ (**6**) is similar to the analogous Al^{III} complex **2** (Scheme 3), apart from the fact that there is only bis-solvation of the Li^+ cation. The lower solvation of the Li^+ cations of **6** results in a polymeric structure in the solid state, as shown by an X-ray structural study of the complex. Attempts to obtain a Ga^{III} derivative by a route similar to that employed for **5** have so far been unsuccessful.

Complexes **2, 3**, **4**, **5**, and **6** were characterized using a combination of elemental analysis, IR and NMR spectroscopy, and X-ray crystallography. All of the complexes are air- and moisture-sensitive, decomposing in a few minutes in air and reacting exothermically with protic solvents. This sensitivity and the tendency to lose THF solvation when placed under vacuum during isolation led to problems in obtaining satisfactory elemental analysis on all the complexes. These problems were compounded in the case of **6**, which is thermally unstable and decomposes slowly under nitrogen atmosphere at room temperature in the solid state or under reflux in THF solution, with the disappearance of the C≡O stretching band in its IR spectrum suggesting attack of the metal-bonded 2-py groups onto the CO ligands. Since the Zn complex **4** could be isolated only in low yield, it was characterized only by X-ray crystallography. The room-temperature ^{1}H NMR spectra of the related Al^{III}/Mo^0 and In^{III}/Mo^0 complexes **2** and **6** (respectively) in benzene reveal the presence of broad pyridyl C−H resonances in the region ca. δ 8.7−6.4, as well as the Me−Al (δ 0.38) or ^{n}Bu−In (δ

(9) Huheey, J. E.; Keiter, E. A.; Keiter, R. L. *Inorganic Chemistry−Principles of Structure and Reactivity*, 4th ed.; pp 114−117.

Scheme 3

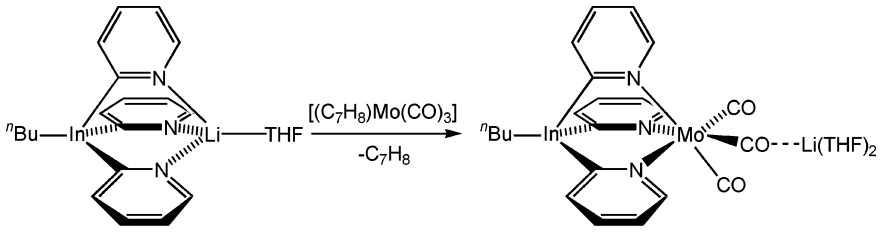

5 **6**

2.44−1.00) resonances for the metal-attached alkyl groups. The IR spectra of solid **2** and **6** both show two major resonances in the CO region, at 1886 (m) and 1873 (s) cm^{-1} in **2** and 1900 (s) and 1890 (sh) cm^{-1} in **6**, which can be assigned tentatively to symmetric and asymmetric stretching bands. It can be noted, however, that there is another minor band present in **2** at 1670 cm^{-1} (absent in **6**). The fact that the IR spectra of both complexes are not altered significantly in THF solution indicates that this minor band is not simply due to ion-pairing with the Li^+ cations in the solid state (see their later structural characterization). The appearance of the IR spectrum of **2** is similar to that of the neutral Sn^{IV} complex [{^{n}BuSn(2-py)$_3$}Mo(CO)$_3$] (with CO stretching bands at 1900, 1788, 1739 cm^{-1} [7c]), and the major bands found in the spectra of **2** and **6** are also similar to those observed in the IR spectrum of the tris-pyrazolylborate complex [TpMo(CO)$_3$]$^-$ [1890 (s), 1750 (vs) cm^{-1}] (Tp = hydridotripyrazolylborato).[10] The similarity of the vibrational frequencies in **2** and **6** suggests that the π-donor/acceptor character of the [MeAl(2-py)$_3$]$^-$ and [^{n}BuIn(2-py)$_3$]$^-$ ligands are similar and affected only to a minor extent by the group 13 metal bridgehead and R group. Bearing this in mind, the large difference in color between them [deep-red for **2**, yellow-brown for **6**] is surprising.

The Ca complex **3** was crystallized as the tris-toluene solvate [**3**·3toluene] from toluene solvent. Elemental analysis and ^{1}H NMR spectroscopy show that this lattice solvation is removed by placing the complex under vacuum (0.1 atm). Repeated analysis, however, gave a C content ca. 2% too low, although the H and N content was as expected for unsolvated **3**. The ^{1}H NMR spectrum of **3** in toluene shows four aromatic C−H resonances for the 2-py group [8.03 (ddd), 7.92 (ddd), 7.09 (dt), 6.33 (ddd)] and the Me resonance for the [MeAl(2-py)$_3$]$^-$ anion as a singlet at δ 0.48. This shows that there is only one solution species present, presumably the *intact*, bis-coordinated structure found later in the solid state. In contrast, the In^{III} complex **5** is clearly highly dynamic in solution, its behavior in toluene solution being very similar to that reported previously for the Al^{III} relative **2**.[8a] At low concentration [0.02 mol L^{-1}] in toluene at room temperature two singlet resonances are observed in the ^{7}Li NMR spectrum, at δ 2.86 and 2.83. However, at higher concentration [0.08 mol L^{-1}] only the resonance at the lower chemical shift is observed. Although the ^{1}H NMR spectra in toluene at both of these concentrations are highly complicated in the aromatic (δ 8.51−6.70) and ^{n}Bu (δ 2.20−0.85) regions, at least two distinct solution species are again apparent, as indicated in particular by the presence of two distinct C(6)−H resonances for the 2-py groups (at δ 8.51 and 8.39) (whose relative integrals are also concentration dependent). These observations suggest that (like **2**[8a]) **5** is involved in a dynamic equilibrium involving loss of THF ligands. Consistent with this hypothesis, the addition of a small amount of THF to a toluene solution of **5** results in simplification of the spectrum, with one dominant species (presumably *intact* **5**) now being apparent in the ^{1}H NMR spectrum [2-py, δ 8.44 [d, C(6)−H], 7.90 (d), 7.12 (mult), 6.72 (mult); ^{n}Bu, 2.50 (mult), 2.00 (mult), 1.65 (t, CH_3), 1.30 (t, α-CH_2)]. Somewhat anomalously, however, the ^{7}Li NMR spectrum still shows at least two dominant solution species at δ 2.94 and 2.25 (298−250 K). In the case of the Al^{III} complex **2**, we were able to isolate and structurally characterize the desolvated species (the dimer [MeAl(2-py)$_3$Li]$_2$), by placing **2** under vacuum at elevated temperature and crystallizing the powder produced from toluene. Unfortunately, similar treatment of **5** resulted in an impure powder that was completely insoluble in nondonor solvents, so could not be characterized by X-ray crystallography or NMR spectroscopy.

The low-temperature X-ray structures of **2**, **3**, **4**, **5**, and **6** were obtained. Details of the data collections and structure refinements of these complexes are given in Table 1. Selected bond lengths and angles for **2**, **3**, **4**, **5**, and **6** are presented in Tables 2, 3, 4, 5, and 6, respectively.

The low-temperature X-ray structure of **2** reveals that the complex is a monomeric, trimetallic species, [{MeAl(2-py)$_3$}-Mo(CO)$_3$Li(THF)$_3$] (**2**), consisting of a [{MeAl(2-py)$_3$}$_2$Mo-(CO)$_3$]$^-$ anion that coordinates a [Li(THF)$_3$]$^+$ cation using one of the O centers of a CO ligand (Figure 2). The structure confirms that the C_7H_8 ligand present in the precursor has been substituted by a [MeAl(2-py)$_3$]$^-$ ligand. The chelation of the Mo center by the three N atoms of this ligand is similar to that observed previously in transition metal complexes [{MeAl(2-py)$_3$}$_2$M] (M = Fe, Mn).[8b] However, **2** is the first transition metal complex in which a low oxidation state, carbonyl fragment is coordinated by this ligand. As such, **2** is related to the previously reported, neutral complex [{^{n}BuSn(2-py)$_3$}Mo(CO)$_3$], which was obtained by substitution of [(THF)Mo(CO)$_5$] by the neutral ligand [^{n}BuSn(2-py)$_3$].[7c]

The bond lengths and angles within the [MeAl(2-py)$_3$]$^-$ ligand of **2** are very similar to those observed previously in the solid-

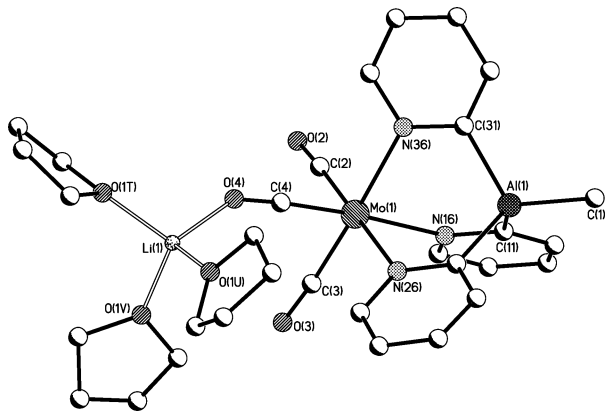

Figure 2. Structure of the trimetallic [{MeAl(2-py)$_3$}Mo(CO)$_3$Li-(THF)$_3$] (**2**). H atoms gave been omitted for clarity.

(10) Curtis, M. D.; Shiu, K.-B. *Inorg. Chem.* **1985**, *24*, 1213.

Table 1. Details of Data Collections and Structural Refinements for [{MeAl(2-py)$_3$}Mo(CO)$_3$Li(THF)$_3$] (2), [{MeAl(2-py)$_3$}$_2$Ca]·3toluene (3·3toluene), [{MeAl(2-py)$_3$}ZnCl] (4), [{^{n}BuIn(2-py)$_3$}Li·THF] (5), and [{^{n}BuInAl(2-py)$_3$}Mo(CO)$_3$Li(THF)$_2$]$_\infty$ (6)

	2	**3**·3toluene	**4**	**5**	**6**
empirical formula	$C_{31}H_{39}AlLiMoN_3O_6$	$C_{53}H_{54}Al_2CaN_6$	$C_{16}H_{15}AlClN_3Zn$	$C_{23}H_{29}InLiN_3O$	$C_{30}H_{37}InLiMoN_3O_5$
fw	679.51	869.06	377.11	485.25	737.33
cryst syst	monoclinic	monoclinic	triclinic	triclinic	monoclinic
space group	*P*2(1)/*c*	*C*2/*c*	$P\bar{1}$	$P\bar{1}$	*P*2(1)/*c*
a (Å)	14.170(3)	9.493(2)	8.558(2)	8.756(2)	17.895(4)
b (Å)	13.738(3)	22.857(5)	9.239(2)	15.522(3)	17.909(4)
c (Å)	18.244(4)	22.727(5)	12.713(3)	17.899(4)	10.100(2)
α (deg)			84.73(3)	74.98(3)	
β (deg)	110.26(3)	94.80(3)	70.83(3)	89.87(3)	99.91(3)
γ (deg)			65.04(3)	84.23(3)	
V (Å^3)	3332(1)	4914 (2)	859.5(4)	2336.8(9)	3189(1)
Z	4	4	2	4	4
F(000)	1408	1840	384	992	1488
cryst size (mm)	0.30 × 0.23 × 0.10	0.16 × 0.12 × 0.12	0.25 × 0.21 × 0.07	0.12 × 0.16 × 0.21	0.10 × 0.16 × 0.18
θ range (deg)	3.57−23.00	3.57−27.47	3.63−25.00	3.541−27.51	3.53−25.00
ρ_{calc} (Mg m^{-3})	1.355	1.175	1.457	1.379	1.536
μ (mm^{-1})	0.464	0.204	1.633	1.028	1.157
no. of reflns collected	21 560	20 493	7522	25 224	22 656
no. of ind reflns	4611	5569	2998	10624	5574
R_{int}	0.046	0.041	0.045	0.042	0.041
absorp corr	multiscan	multiscan	multiscan	multiscan	multiscan
max., min. transmn	0.930/0.843	0.980/0.949	0.892/0.671	0.884/0.821	0.891/0.812
no. of data/restraints/ params	4611/0/389	5569/0/299	2998/0/200	10 624/10/498	5574/0/368
goodness-of-fit on F^2	1.040	1.024	1.147	1.049	1.009
R indices ($I > 2\sigma I$)	$R_1 = 0.032$, $wR_2 = 0.088$	$R_1 = 0.049$, $wR_2 = 0.121$	$R_1 = 0.056$, $wR_2 = 0.126$	$R_1 = 0.047$, $wR_2 = 0.120$	$R_1 = 0.032$, $wR_2 = 0.069$
R indices (all data)	$R_1 = 0.040$ $wR_2 = 0.092$	$R_1 = 0.067$ $wR_2 = 0.131$	$R_1 = 0.0731$ $wR_2 = 0.1301$	$R_1 = 0.073$ $wR_2 = 0.135$	$R_1 = 0.046$ $wR_2 = 0.073$
largest peak and hole (e Å^{-3})	0.368/−0.493	0.893/−0.500	0.546/−0.550	1.456/−1.397	0.604/−0.388

[a] Data in common; $\lambda = 0.71073$ nm, $T = 180(2)$ K.

Table 2. Selected Bond Lengths and Angles for [{MeAl(2-py)$_3$}Mo(CO)$_3$Li(THF)$_3$] (2)

Bond Lengths (Å)

C(1)−Al(1)	1.976(4)	Mo(1)−C(3)	1.948(4)
Al(1)−C(11)	1.977(3)	Mo(1)−C(2)	1.952(3)
Al(1)−C(21)	1.968(3)	C(2)−O(2)	1.165(4)
Al(1)−C(31)	1.971(3)	C(3)−O(3)	1.170(4)
N(16)−Mo(1)	2.335(2)	C(4)−O(4)	1.195(3)
N(26)−Mo(1)	2.305(2)	O(4)−Li(1)	1.926(6)
N(36)−Mo(1)	2.313(3)	Li−O(1T,1U,1V)	1.911(6)−1.925(6)
Mo(1)−C(4)	1.910(3)	Mo(1)···Al(1)	3.532(1)

Bond Angles (deg)

C_α−Al(1)−C(1)[a]	112.5(2)−115.0(2)	C(4)−Mo(1)−C(2)	90.5(1)
C_α−Al(1)−C_α	104.3(1)−105.2(1)	C(4)−Mo(1)−C(3)	85.6(1)
C_α−N−Mo(1)	av 123.6	N−Mo(1)−C(2,3,4)	90.0(1)−95.5(1)
N(26)−Mo(1)−N(16)	87.81(9)	C(4)−O(4)−Li(1)	146.3(3)
N(36)−Mo(1)−N(16)	89.09(9)		
N(26)−Mo(1)−N(36)	88.53(9)		
C(3)−Mo(1)−C(2)	84.1(1)		

[a] C_α are the α-C atoms of the 2-pyridyl groups [C(11), C(21), C(31)].

Table 3. Selected Bond Lengths and Angles for [{MeAl(2-py)$_3$}$_2$Ca] (3)

Bond Lengths (Å)

C(1)−Al(1)	1.978(2)	N(16)−Ca(1)	2.481(2)
Al(1)−C(11)	2.024(2)	N(26)−Ca(1)	2.476(2)
Al(1)−C(21)	2.015(2)	N(36)−Ca(1)	2.489(2)
Al(1)−C(31)	2.023(2)	Al(1)···Ca(1)	3.630(1)

Bond Angles (deg)

C_α−Al(1)−C(1)[a]	112.44(9)−113.75(9)	Al(1)−C_α−N	av 118.4
C_α−Al(1)−C_α	105.36(8)−106.66(8)	N−Ca(1)−N range	87.41(5)−92.59(5)

[a] C_α are the α-C atoms of the 2-pyridyl groups [C(11), C(21), C(31)].

state structures of other complexes containing this ligand. In particular, the range of angles at the Al(III) bridgehead in **2** [C_α−Al(1)−C_α 104.3(1)−105.2(1)°] closely matches the ranges found in both transition metal and lithium complexes of this type [101.8(1)−104.7(2)°],[8] suggesting little strain results from the coordination even of a large Mo^0 center. The coordination of this Mo^0 in **2** by the three N atoms of the 2-py groups is not entirely regular [Mo(1)−N(16,26,36) range 2.305(2)−2.335(2) Å], and it is noticeable that the longest Mo−N bond [N(16)−Mo(1) 2.335(2) Å] appears to give rise to a short, *trans*-Mo−C

Table 4. Selected Bond Lengths and Angles for the Disordered Molecule [MeAl(2-py)$_3$}ZnCl] (4)

Bond Lengths (Å)			
Al(1)−C(1)	2.075(5)	Zn(1)−Cl(1)	2.210(2)
Al(1)−C(11)	2.019(5)	N(16)−Zn(1)	2.034(4)
Al(1)−C(21)	2.009(5)	N(26)−Zn(1)	2.043(4)
Al(1)−C(31)	1.999(5)	N(36)−Zn(1)	2.021(5)
		Zn(1)···Al(1)	
Bond Angles (deg)			
C(1)−Al(1)−C$_\alpha$[a]	111.2(2)−118.2(2)	N(3)−Zn(1)−N(2)	104.2(2)
C$_\alpha$−Al(1)−C$_\alpha$	100.1(2)−104.1(2)	N(1)−Zn(1)−N(2)	97.9(2)
N(3)−Zn(1)−N(1)	103.3(2)	N−Zn(1)−Cl(1)	112.4(1)−115.1(1)

[a] C$_\alpha$ are the α-C atoms of the 2-pyridyl groups [C(11), C(21), C(31)].

Table 5. Selected Bond Lengths and Angles for [^{n}BuIn(2-py)$_3$Li·THF] (5)

Bond Lengths (Å)			
In(1)−C(1)	2.186(5) [2.169(5)][a]	In(1)···Li(1)	3.157(6) [3.126(6)]
In(1)−Cα[b]	2.211(4)−2.222(4) [2.215(4)−2.224(4)]	Li(1)−O$_{(THF)}$	1.996(6) [2.001(7)]
N$_{(py)}$−Li	2.057(6)−2.082(6) [2.050(6)−2.081(6)]		
Bond Angles (deg)			
C(1)−In(1)−C$_\alpha$	114.6(2)−119.7(2) [115.9(2)−118.5(2)]	N$_{(py)}$−Li(1)−N$_{(py)}$	105.4(3)−107.5(3) [104.1(3)−108.5(4)]
C$_\alpha$−In(1)−C$_\alpha$	100.3(2)−101.8(2) [97.6(1)−102.6(1)]	N$_{(py)}$−Li(1)−O$_{(THF)}$	107.3(9)−114.2(3) [109.0(3)−116.0(4)]

[a] Values in parentheses are for molecule B. [b] C$_\alpha$ are the α-C atoms of the 2-pyridyl groups [C(11), C(21), C(31)].

Table 6. Selected Bond Lengths and Angles for [{^{n}BuIn(2-py)$_3$}Mo(CO)$_3$Li(THF)$_2$]$_\infty$ (6)

Bond Lengths (Å)			
In(1)−C(1)	2.196(3)	Mo(1)−C(3)	1.908(4)
In(1)−C(11)	2.187(3)	Mo(1)−C(2)	1.949(4)
In(1)−C(21)	2.197(4)	C(2)−O(2)	1.164(4)
In(1)−C(31)	2.197(3)	C(3)−O(3)	1.181(4)
N(16)−Mo(1)	2.343(3)	C(4)−O(1B)	1.189(4)
N(26)−Mo(1)	2.338(3)	O(3)−Li	1.926(6)
N(36)−Mo(1)	2.337(3)	O(1)−Li	1.900(6)
Mo(1)−C(4)	1.905(4)	Li−O(THF) (mean)	1.926(6)
		Mo(1)···In(1)	3.724(1)
Bond Angles (deg)			
C$_\alpha$−In(1)−C(1)[a]	113.8(2)−120.9(1)	C(4)−Mo(1)−C(3)	80.9(2)
C$_\alpha$−In(1)−C$_\alpha$	98.5(1)−101.5(1)	N−Mo(1)−C(2,3,4)	91.4(1)−94.9(1)
C$_\alpha$−N−Mo(1)	av 125.6	C(4)−O(1B)−LiB	167.5(3)
N(26)−Mo(1)−N(16)	92.1(1)	O(1B)−LiB−O(3B)	117.3(3)
N(36)−Mo(1)−N(16)	90.2(1)	C(3)−O(3)−Li	159.4(3)
N(26)−Mo(1)−N(36)	89.5(1)	O(3)−Li−O(1)	117.5(3)
C(3)−Mo(1)−C(2)	84.0(1)		
C(4)−Mo(1)−C(2)	84.1(1)		

[a] C$_\alpha$ are the α-C atoms of the 2-pyridyl groups [C(11), C(21), C(31)].

bond [Mo(1)−C(4) 1.910(3) Å]. At first sight this pattern of bond lengths might be taken to suggest a *trans*-influence of the pyridyl-N metal bonding on the metal carbonyl bonding, i.e., that as the extent of bonding of the p orbital of the pyridyl-N atom with the Mo (d_{xy}, d_{xz}, or d_{yz}) orbitals decreases, a greater extent of back-bonding to the *trans*-CO ligand would be expected. However, this does not seem to be the case, as no such correlation between the Mo−N and Mo−C bond lengths is discernible in the structure of the closely related complex [{^{n}BuIn(2-py)$_3$}Mo(CO)$_3$Li(THF)$_2$]$_\infty$ (**6**) (see later discussion, Figure 6). Rather, the common effect in both **2** and **6** is the influence of the Li^+ cations on the pattern of carbonyl bonding. In **2**, the result of bonding of the Li^+ cation to O(4) is to lengthen the C−O bond of the carbonyl ligand [C(4)−O(4) 1.195(3) Å] and shorten the associated C−Mo bond [Mo(1)−C(4) 1.910(3) Å] [cf. 1.165(4)−1.170(4) Å and 1.948(3)−1.952(4) Å for the other C−O and Mo−C bonds, respectively, in **2**]. The same effect is also seen in **6**, in which two of the longest C−O bonds are associated with the CO ligands bonded to the Li^+ cations [C−O(1B,3) 1.181(4)−1.189(4) Å; cf. C(2)−O(2) 1.164(4) Å], with the corresponding Mo−C bond lengths being the shortest [Mo(1)−C(3,4) 1.903(4)−1.908(4) Å; cf. 1.949(4) Å]. This pattern of C−O and Mo−C bond lengths can be explained by a classical resonance model in which transfer of electron density from Mo to the CO ligand results in transfer of negative charge to the O atom, optimizing O−Li bonding. The observation of CO−Li bonding in **2** and **6** is not unusual.[11] A large number of alkali and alkaline earth complexes of this type have been reported previously.[12]

(11) Wong, W.-T.; Wong, W.-K. *Acta Crystallogr.* **1994**, *50C*, 1404. Leiner, E.; Hampe, O.; Scheer, M. *Eur. J. Inorg. Chem.* **2002**, 584. Fretzen, A.; Ripa, A.; Liu, R.; Bernardinelli, G.; Kundig, E. P. *Chem. Eur. J.* **1998**, *4*, 251. Heyn, R. H.; Huffman, J. C.; Caulton, K. G. *New J. Chem.* **1993**, *17*, 797. Neumüller, B.; Petz, W. *Organometallics* **2001**, *20*, 163. Balema, V.; Goesmann, H.; Materu, W.; Fritz, G. *Z. Anorg. Allg. Chem.* **1996**, *35*, 622. Hou, H.; Rheingold, A. L.; Kubiak, C. P. *Organometallics* **2005**, *24*, 231.

(12) Conquest software for searching the Cambridge Structural Data Base and Visualizing Crystal Structures (January 2006). Bruno, I. J.; Cole, J. C.; Edgington, P. R.; Kessler, M.; Macrae, C. F.; McCabe, P.; Pearson, J.; Taylor, R. *Acta Crystallogr.* **2001**, *B58*, 389.

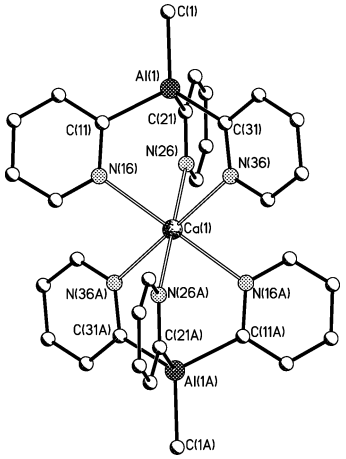

Figure 3. Structure of [{MeAl(2-py)$_3$}$_2$Ca] (**3**). H atoms and toluene molecules in the lattice have been omitted for clarity. Symmetry A: $1.5 - x$, $0.5 - y$, $-z$.

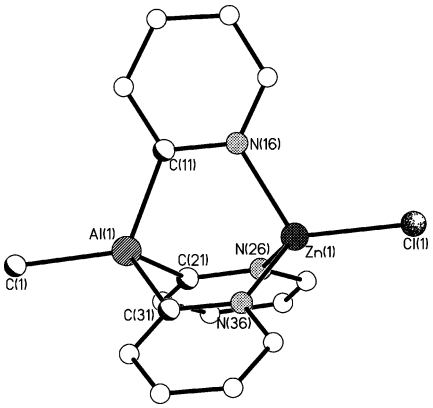

Figure 4. Structure of the monomeric molecule of [MeAl(2-py)$_3$}-ZnCl] (**4**) illustrated by the 80% component of the disorder. H atoms have been omitted for clarity.

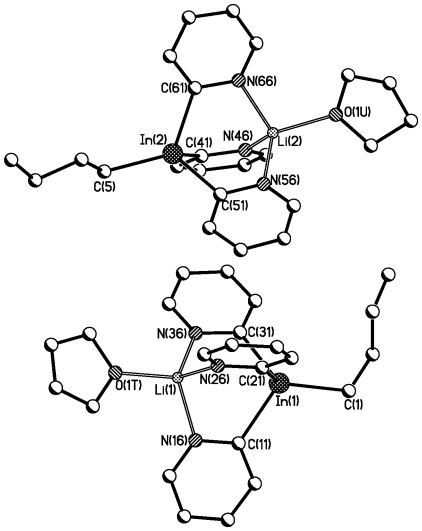

Figure 5. The two independent molecules of [{^{n}BuIn(2-py)$_3$}Li·THF] (**5**) present in the unit cell. H atoms have been omitted for clarity.

The structure of **3** (Figure 3) is that of a monomer of formula [{MeAl(2-py)$_3$}$_2$Ca], in which the Ca^{2+} ion is coordinated by two [MeAl(2-py)$_3$]$^-$ anions. The Ca^{2+} ion is coordinated by six N atoms of the two tris-pyridyl ligands [N−Ca range 2.476(2)−2.489(2) Å] in an almost regular octahedral geometry [N−Ca(1)−N range 87.41(5)−92.59(5)°]. The structural arrangement of **3** is the same as that observed previously for [{MeAl(2-py)}$_2$M] (M = Fe^{II}, Mn^{II}).[8b] The bond lengths and angles found in the [MeAl(2-py)$_3$]$^-$ anions in **3** are very similar to those found in these complexes [Al−C range 1.978(2)−2.023(2) Å, C_α−Al(1)−C_α 105.36(8)−106.66(8)° in **3**; cf. 1.969(3)−2.014(3) Å, C_α−Al(1)−C_α 104.3(1)−105.2(1)° for the corresponding values in [{MeAl(2-py)}$_2$M] (M = Fe^{II}, Mn^{II})[8b]]. The Ca−N bonds in **3** [range 2.476(2)−2.489(2) Å] are in the range found previously in Ca−N bonded complexes [mean 2.52 Å].[12]

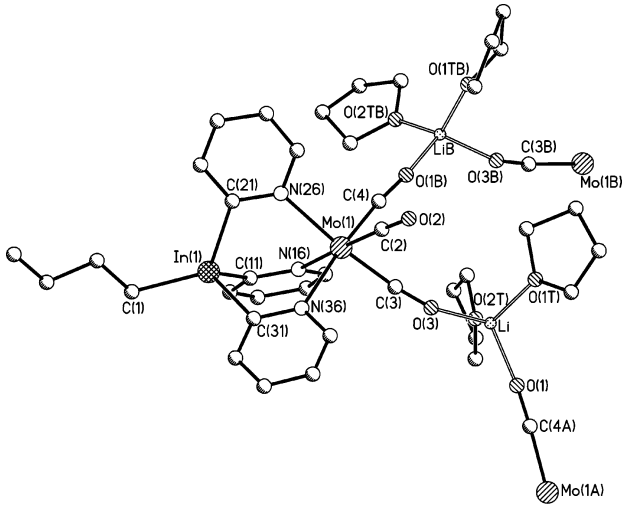

Figure 6. Part of the polymeric structure [{^{n}BuIn(2-py)$_3$}Mo(CO)$_3$Li(THF)$_2$]$_\infty$ (**6**): symmetry A x, $1.5 - y$, $-0.5 + z$; B x, $1.5 - y$, $0.5 + z$.

The structure of **4** is that of a simple monomer [{MeAl(2-py)$_3$}ZnCl], in which the pseudotetrahedral Zn^{2+} ion is coordinated by one [MeAl(2-py)$_3$]$^-$ ligand (Figure 4). Molecules of **4** exhibit unusual crystallographic disorder about a virtual inversion center between the Zn and Al atoms so the metal atom positions shown in Figure 5 are Zn(1) 80:20% Zn:Al and Al(1) 20:80% Zn:Al (with the 2-py and Me groups and Cl atom also being similarly disordered). As a result of this disorder, meaningful discussion of the bond lengths and angles in **4** is not possible.

Monomeric molecules of **5** are directly related to the structure of the Al^{III} precursor [{MeAl(2-py)$_3$}Li·THF] (**1**), being an ion-paired complex composed of the [^{n}BuIn(2-py)$_3$]$^-$ anion coordinated to a THF-solvated Li^+ cation (Figure 5). There are two chemically identical but crystallographically independent molecules present in the unit cell (Figure 5). Table 5 includes selected bond lengths and angles for both independent molecules. However, the following discussion will concern averages or ranges of bond lengths and angles for both forms. The most obvious effect of changing the bridgehead atom from Al to In is an increase in the ligand bite. Although there is a small reduction in the bridgehead C_α−In−C_α angle [range 100.2(1)−102.6(2)° in **5**; cf 103.83(9)−104.4(1)° in **1**[8a]], which would tend to reduce the ligand bite compared to the related Al^{III} complex, the major factor dictating the ligand bite is the increase in the C_α−metal bond length. Thus, in **5** the C_α−In bond lengths [2.207(4)−2.226(4) Å] are ca. 0.2 Å longer than the C_α−Al bonds in **1**, resulting in a net increase in the bite from 3.23 Å in **1**[8a] to 3.34 Å in **5** (in both cases expressed as the mean N···N separation). The dominant influence of the C_α−metal bond length on the ligand bite is the same as that found for the neutral counterparts [MeE(2-py)$_3$] (E = C,[3] Si,[7c] Sn[7a,b]) as group 14 is descended.

The structure of the trimetallic complex $[\{^n\text{BuIn}(2\text{-py})_3\}\text{Mo}(\text{CO})_3\text{Li}(\text{THF})_2]_\infty$ (**6**) is very similar to that of the Al^{III} complex **2** (Figure 6), the major difference being that the Li^+ cation in **6** is only bis-coordinated by THF ligands (as a opposed to being tris-coordinated as in **2**). This difference results in a polymeric structure for **6** in which molecules are linked together, via C≡O···Li···O≡C bridges, into a zigzag arrangement generated by the *c*-glide. The reason for this difference is probably steric in origin, in particular stemming from the presence of an ^{n}Bu group on the In^{III} center in **6** as opposed to a Me group in **2**. The bond lengths and angles within the $[^n\text{BuIn}(2\text{-py})_3]^-$ anion of **6** are very similar to those found in the structure of the precursor **5** [e.g., In−C range 2.186(4)−2.197(4) Å, C_α−In(1)−C_α 98.5(1)−101.4(1)° in **6**; cf 2.159(5)−2.226(4) Å, 97.5(1)−102.6(2)° in **5**]. The Mo−N and Mo−C bond lengths in **6** [Mo(1)−N range 2.337(3)−2.343(3) Å, Mo(1)−C range 1.903(4)−1.952(4) Å] are similar to those found in the related Al^{III} complex **2**.

Conclusions

The results reported here and by us previously[8] show that group 13 tris-pyridyl ligands of the type $[\text{RE}(2\text{-py})_3]^-$ have broad applications in coordination chemistry, in the coordination of harder main group metal ions (Li^+, Ca^{2+}, Zn^{2+}), and for higher (Mn^{II}, Fe^{II}) and lower oxidation state [Mo^0] transition metals. Future studies will be aimed at exploring the electrochemical activity of the group 13 bridgehead atoms in various complexes (especially transition metal complexes) and the potential catalytic activity of these species. A further direction of interest to us in future studies is the formation of related 3- and 4-pyridyl derivatives and the exploration of the potential supramolecular chemistry of these ligands.

Experimental Section

General Procedures. Compounds **2**, **3**, **4**, **5**, and **6** are air- and moisture-sensitive. They were handled on a vacuum line (in an efficient cupboard) using standard inert-atmosphere techniques and under dry/oxygen-free argon. 2-Bromopyridine, $ZnCl_2$ (99.99%), $InCl_3$ (99%), and CaI_2 (99.9%) were acquired from Aldrich Chemical Co. 2-Bromopyridine was freshly distilled over CaH_2 prior to lithiation reactions. $[(C_7H_8)\text{Mo}(\text{CO})_3]$ was prepared by the literature route.[13] THF was dried by distillation over sodium/benzophenone prior to the reactions. The products were isolated and characterized with the aid of an argon-filled glovebox fitted with a Belle Technology O_2 and H_2O internal recirculation system. Melting points were determined by using a conventional apparatus and sealing samples in capillaries under argon. IR spectra were recorded as Nujol mulls using NaCl plates and were run on a Perkin-Elmer Paragon 1000 FTIR spectrophotometer. Elemental analyses were performed by first sealing the samples under argon in airtight aluminum boats (1−2 mg), and C, H, and N content was analyzed using an Exeter Analytical CE-440 elemental analyzer. ^{1}H, ^{13}C, and ^{7}Li NMR spectra were recorded on a Bruker DPX 400 MHz spectrometer in dry benzene or toluene (using the solvent resonances as the internal reference standard for ^{1}H and ^{13}C studies and a saturated solution of $LiCl/D_2O$ as the external standard for ^{7}Li NMR studies). The synthesis of **1** has been described elsewhere. Details of the syntheses only of the new compounds (**2**−**6**) are reported here.

Synthesis of 2. Solid cycloheptatrienylmolybdenum tricarbonyl, $[(C_7H_8)\text{Mo}(\text{CO})_3]$ (0.272 g, 1.0 mmol), was added to a solution of **1** in THF (20 mL) at room temperature. The mixture was stirred at room temperature (2 h), resulting in the dark red color of the starting solution of $[(C_7H_8)\text{Mo}(\text{CO})_3]$ intensifying. The solvent was removed under vacuum, together with any volatile products. The residue was dissolved in THF (15 mL) and the solution stored at −5 °C (1 week) to give red, hexagonal plates (0.45 g, 0.66 mmol, 66%). Decomposition ca. 125 °C to black solid. IR (solid, Nujol, NaCl): ν/cm^{-1} 1886 (m), 1873 (s) (CO str). ^{1}H NMR (500.2 MHz, d_6-benzene, +25 °C): δ/ppm 8.65 [br d, 3H, C(5)−H], 6.75 [br s, C(3,4)−H, 6H], 6.42 [br s, 3H, C(2)−H], 3.70 [m, 4H, $-CH_2-$O, THF], 1.52 [m, 4H, $-CH_2-$, THF], 0.38 [s, 3H, Me−Al]. ^{7}Li NMR (194.40 MHz, d_6-benzene, +25 °C, rel to saturated $LiCl/D_2O$): δ/ppm −0.58. Anal. Found: 54.6, H 5.6, N 6.3. Calcd for **2**: C 54.8, H 5.7, N 6.2.

Synthesis of 3. A mixture of CaI_2 (0.5 mmol) and **1** (0.355 g, 1.0 mmol) was dissolved in toluene (30 mL). The mixture was stirred at room temperature for 3 days to give a yellow solution with a fine white precipitate. The mixture was filtered through Celite, and the volume of solvent was reduced under vacuum to ca. 10 mL. The filtrate was stored at −20 °C for 2 days to give colorless, rectangular crystals. X-ray crystallography showed that these are the tris-solvate **3**·3toluene. Placing the crystals under vacuum during isolation (10^{-1} atm, 15 min) removed almost all of the lattice-bound toluene and resulted in the formation of an amorphous powder of **3**. The following data refer to this material. Yield: 0.15 g, 51%). Decomposition ca. 300 °C to black solid. ^{1}H NMR (500.2 MHz, d_6-toluene, +25 °C): δ/ppm 8.03 (ddd, 6H, C(5)−H, J = 7.4 Hz, J = 1.2 Hz, J = 1.2 Hz), 7.92 (ddd, 6H, C(3)−H, J = 5.2, J = 1.6, J = 1.2 Hz), 7.09 (dt, 6H, C(4)−H, J = 7.6, J = 1.7 Hz), 6.33 (ddd, 6H, C(2)−H, J = 7.6, J = 5.2, J = 1.5 Hz), 0.48 (s, 6H, CH_3-Al). Anal. Found: C 62.8, H 5.4, N 14.1. Calcd for **3**: C 64.8, H 5.1, N 14.2.

Synthesis of 4. A mixture of solid $ZnCl_2$ (0.134 g, 1.0 mmol) and **1** (0.355 g, 1.0 mmol) was dissolved in THF (10 mL) and brought to reflux (2 h). The volume of the resulting orange solution was then reduced under vacuum to ca. 4 mL and the solution stored at 5 °C for 48 h to give a few colorless needles of **4**. Owing to the very low yield of the complex, it could be characterized only by X-ray crystallography.

Synthesis of 5. To a solution of $InCl_3$ (2.21 g, 10 mmol) in THF (40 mL) was added ^{n}BuLi (6.25 mL, 1.6 mol dm^{-3} in hexanes, 10 mmol) dropwise at −78 °C. The reaction mixture was stirred at room temperature (2 h) to give a clear, colorless solution. This solution was added dropwise to a solution of 2-Li-py [obtained by the addition of ^{n}BuLi (18.75 mL, 1.6 mol dm^{-3} in hexanes, 30 mmol) to 2-Br-py (2.85 mL, 30 mmol) in THF (100 mL) at −78 °C (stirred for 3 h)]. The reaction mixture was allowed to warm to room temperature, then stirred (16 h), producing a gray suspension. The solvent was removed under vacuum and the residue extracted with *n*-pentane (60 mL) and filtered. The volume of the residue was reduced under vacuum until precipitation occurred. The precipitate was dissolved by heating gently. Storage at room temperature (16 h) gave colorless crystalline blocks of **5** (0.67 g, 13%; the reaction can be scaled up to 20 mmol with only a small reduction in the yield). IR (solid, Nujol, NaCl): ν/cm^{-1} 3028 (w) (aryl C−H). ^{1}H NMR (500.2 MHz, d_6-benzene, +25 °C): δ/ppm 8.51 (dd, C(6)−H 2-py), 8.39 (d, C(6)−H, 2-py), 7.59 (mult, 2-py), 7.15 (mult 2-py), 6.70 (mult, 2-py) (total integral 12H), 3.60 (mult, 4H, THF), 1.49 (mult, 4H, THF), 2.20−0.85 (overlapping mult, 9H, ^{n}Bu). ^{7}Li (194.40 MHz, d_6-benzene, +25 °C, rel to saturated $LiCl/D_2O$): δ/ppm 2.86 (s), 2.83 (s) [0.02 mol L^{-1}], 2.83 (s) [0.08 mol L^{-1}]. Anal. Found: C 56.0, H 5.9, N 8.6. Calcd for **5**, C 56.9, H 6.0, N 8.7.

Synthesis of 6. To a solution of **5** (0.295 g, 0.61 mmol) in THF (10 mL) at room temperature was added solid $[(C_7H_8)\text{Mo}(\text{CO})_3]$ (0.166 g, 0.61 mmol). The reaction changed color from deep red to brown-yellow over the course of 1 h. Stirring was continued for a further 1 h before the solvent was removed under vacuum and the oily solid pumped on for ca. 1 h to remove volatile components.

(13) Hooker, R. H.; Rest, A. J. *J. Chem. Soc., Dalton Trans.* **1982**, 2029.

This was then washed with hexane (2 × 10 mL) and the yellow-brown powder of **6** dried under vacuum (10^{-1} atm, 15 min). This treatment resulted in the loss of ca. 0.5−1.0 of the coordinated THF ligands. The following data refer to this material. Yield: 0.31g (69%). IR (solid, Nujol, NaCl): ν/cm^{-1} 1890 (s), 1890 (m) (CO str). ^{1}H NMR (500.2 MHz, d_6-benzene, +25 °C): δ/ppm 8.52 [br s, 3H, C(5)−H], 7.20 [t, 3H, C(3,4)−H], 6.65 [t, 3H, C(2)−H], 3.63 [m, ca. 5.8H, $-CH_2-O$, THF], 1.43 [m, ca. 5.8H, $-CH_2-$, THF], 2.46−1.00 [overlapping mults, 9H, ^{n}Bu-In]. ^{7}Li (194.40 MHz, d_6-benzene, +25 °C, rel to saturated LiCl/D_2O): δ/ppm −0.50 (s). Anal. Found: C 46.3, H 4.8, N 5.4. Calcd for **6**-THF: C 46.9, H 4.4, N 6.3. Crystals of **6** were grown by storage of a THF solution of **6** for several weeks (−15 °C).

Crystal Structures of 2−6. Crystals of **2**−**6** were mounted directly from solution under argon using an inert oil, which protects them from atmospheric oxygen and moisture. X-ray intensity data were collected using a Nonius Kappa CCD diffractometer. Details of the data collections and structural refinements are given in Table 1. For all the crystals the positions of the non-hydrogen atoms were located by direct methods and refinement was based on F^2.[14] In the crystals of compounds **3** the Ca(1) atom is on an inversion center, so the overall molecular structure has crystallographic C_i symmetry. There are also three half toluene solvates per asymmetric unit, two across C_2 axes and the third disordered across an inversion center. Throughout the crystal of **4** there is a random distribution of two orientations of the molecule, which superimpose almost exactly so that there is 80:20 disorder at each site, with Al superimposed on Zn and vice versa, with a corresponding disorder of the donor atoms. The bond lengths therefore cannot be discussed meaningfully, but the overall structure is well established. In the crystals of **5** there are two independent molecules per equivalent position that are chemically identical and approximately related by a noncrystallographic inversion center broken only by the atoms of the butyl ligands, which are in different orientations. To minimize the effects of correlation, the pairs of approximately centrosymmetrically related bond lengths of the coordination spheres of the two independent molecules were constrained to be equal within an esd of 0.01 Å. Relatively high atomic displacement parameters indicate some conformational disorder of the THF ligands in **2**, **5**, and **6** and of the ^{n}Bu ligands in **5** and **6**. This disorder was only resolved for one ^{n}Bu C atom (70:30%) in **5** and two THF C atoms (50:50) in **6**. The hydrogen atoms for all five structures were placed in calculated positions with displacement parameters set equal to $1.2U_{eq}$ (or $1.5U_{eq}$) for methyl groups of the parent carbon atoms. In the final cycles of full-matrix least-squares refinement, the non-hydrogen full-occupancy atoms were assigned anisotropic displacement parameters. Atomic coordinates, bond lengths and angles, and thermal parameters for **2**, **3**, **4**, **5**, and **6** have been deposited with the Cambridge Crystallographic Data Centre.

(14) Sheldrick, G. M. *SHELX-97*; Göttingen, 1997.

Acknowledgment. We thank the EPSRC (F.G., R.A.K., M.C.R., M.McP., D.S.W.), Churchill and Fitzwilliam Colleges (Fellowship for A.D.H.), Wolfson College (Fellowship for F.G.), and Churchill College (Winston Churchill Fellowship for J.S.S.) for financial support.

Supporting Information Available: Full listings of X-ray crystallographic data, atomic coordinates, thermal parameters, bond distances, bond angles, and hydrogen parameters for **2**, **3**, **4**, **5**, and **6**. This material is available free of charge via the Internet at http://pubs.acs.org.

OM0600691